- 1 BMI-1 extends proliferative potential of human bronchial epithelial cells whilst
- 2 retaining their mucociliary differentiation capacity.
- 3 Mustafa M. Munye¹; Amelia Shoemark²; Robert A. Hirst³; Juliette M. Delhove¹; Tyson
- 4 V. Sharp⁴; Tristan R. McKay⁵; Christopher O'Callaghan¹; Deborah L. Baines⁶;
- 5 Steven J. Howe¹; Stephen L. Hart¹

6 **AFFILIATIONS**

- ⁷ ¹ UCL Great Ormond Street Institute of Child Health, London, United Kingdom.
- ⁸ ² Imperial College London, UK Electron Microscopy Dept, Royal Brompton and
- 9 Harefield NHS Foundation Trust, London, UK.
- ³ Primary Ciliary Dyskinesia Centre Department of Infection, Immunity and
- 11 Inflammation, University of Leicester, Leicester, United Kingdom.
- ⁴ Centre for Molecular Oncology, Barts Cancer Institute, Queen Mary University of
- 13 London, London, United Kingdom.
- ¹⁴ ⁵ School of Healthcare Science, Manchester Metropolitan University, Manchester,
- 15 United Kingdom.
- ⁶ Institute for Infection and Immunity, St George's, University of London, London,
- 17 United Kingdom
- 18
- 19 Correspondence should be addressed to M.M.M. (m.munye@ucl.ac.uk)
- 20 UCL Institute of Child Health, 30 Guilford Street, London, WC1N 1EH, United
- 21 Kingdom

22 ABBREVIATIONS LIST

- 23
- 24 ALI = Air-Liquid Interface
- 25 BEGM = Bronchial Epithelial Growth Media
- 26 CBF = Cilia Beat Frequency
- 27 CFBE = Cystic Fibrosis Bronchial Epithelial
- 28 CRCs = Conditionally Reprogrammed Cells
- 29 DMEM = Dulbecco's Modified Eagle Medium
- 30 GFP = Green Fluorescent Protein
- 31 HBE = Human Bronchial Epithelial
- 32 hESCs = human Embryonic Stem Cells
- 33 hTERT = human Telomerase Reverse Transcriptase
- 34 iPSCs = induced Pluripotent Stem Cells
- I_{sc} = short circuit current
- 36 NHBE = Normal Human Bronchial Epithelial
- 37 ODA = Outer Dynein Arms
- 38 PBS = Phosphate Buffered Saline
- 39 PCD = Primary Ciliary Dyskinesia
- 40 ROCK = Rho-associated protein kinase

41 **ABSTRACT**

42 Air-liquid interface (ALI) culture of primary airway epithelial cells enables mucociliary 43 differentiation providing an *in vitro* model of the human airway but their proliferative 44 potential is limited. To extend proliferation, these cells were previously transduced 45 with viral oncogenes or mouse Bmi-1 + hTERT but the resultant cell lines did not 46 undergo mucociliary differentiation. We hypothesised that use of human BMI-1 alone 47 would increase the proliferative potential of bronchial epithelial cells while retaining 48 their mucociliary differentiation potential. CF and non-CF bronchial epithelial cells 49 were transduced by lentivirus with *BMI-1* then their morphology, replication kinetics 50 and karyotype were assessed. When differentiated at ALI, mucin production, ciliary 51 function and transepithelial electrophysiology were measured. Finally, shRNA 52 knockdown of DNAH5 in BMI-1 cells was used to model primary ciliary dyskinesia 53 (PCD). BMI-1 transduced basal cells showed normal cell morphology, karyotype 54 and doubling times despite extensive passaging. The cell lines underwent 55 mucociliary differentiation when cultured at ALI with abundant ciliation and 56 production of the gel-forming mucins MUC5AC and MUC5B evident. Cilia displayed 57 a normal beat frequency and 9+2 ultrastructure. Electrophysiological characteristics 58 of BMI-1 transduced cells were similar to un-transduced cells. shRNA knockdown of 59 DNAH5 in BMI-1 cells produced immotile cilia and absence of DNAH5 in the ciliary 60 axoneme as seen in cells from patients with PCD. BMI-1 delayed senescence in 61 bronchial epithelial cells, increasing their proliferative potential but maintaining 62 mucociliary differentiation at ALI. We have shown these cells are amenable to 63 genetic manipulation and can be used to produce novel disease models for research 64 and dissemination.

- 65 Key words: air-liquid interface, airway model, lung, mucociliary differentiation,
- 66 primary ciliary dyskinesia

67 **INTRODUCTION**

The ciliated epithelium lining the airways provides the first line of defence to inhaled pathogens and particles and plays a crucial role in many respiratory diseases. It is possible to remove respiratory epithelial cells from the nose or upper airways of donors by brushing and culture them in the laboratory on collagen-coated, semi-permeable membranes. The progenitor basal epithelial cells from the brushings cultured at Air-Liquid Interface (ALI) differentiate into a fully ciliated, pseudostratified epithelium closely resembling that found in the airway (3).

75 If cells are obtained from a donor with a lung disease, e.g., cystic fibrosis, primary ciliary 76 dyskinesia (PCD), asthma and chronic obstructive pulmonary disease, these ALI cultures 77 provide a surrogate model of the diseased lung for research into pathogenic mechanisms 78 and for the development of new therapeutics(9, 14, 16). However, basal epithelial cells can 79 only be passaged 2-3 times before they lose their proliferation and differentiation potential 80 (6, 18). Thus, to establish the wider use of basal cells in ALI epithelial culture models, 81 methods are required that enable basal cells to be cultured for longer, genetically 82 engineered, expanded and stored easily prior to differentiation on ALI cultures. Such cells 83 would also overcome ethical issues related to repeated brushing of volunteers.

84 Recent approaches to extend the utility of primary, basal epithelial cells involved culturing 85 them with rho-associated protein kinase (ROCK) inhibitors on a layer of irradiated feeder 86 cells to provide cell-derived growth factors (18, 27). The requirement for irradiated feeder 87 cells makes the maintenance of basal cell cultures complex and time-consuming, difficult to 88 scale up and may limit the use of this approach to specialist laboratories. Alternatively, 89 induced pluripotent stem cells (iPSCs) and embryonic stem cells (hESCs) were differentiated 90 into mature respiratory epithelial cells and used to generate a pseudostratified epithelium 91 expressing CFTR (30). However, the process takes several weeks and often the resulting 92 cultures are not suitable for disease modelling as they are contaminated with endodermal

cell types (31) and often present with karyotypic anomalies which may confound drug
 screening efforts.

95 Extended proliferative potential of primary human bronchial epithelial (HBE) cells 96 was described by transduction of basal cells with the mouse polycomb complex 97 protein *Bmi-1* and human telomerase reverse transcriptase (*hTERT*) (6). Unlike cells 98 transformed with viral oncogenes, Bmi-1+hTERT cell lines had no chromosomal 99 abnormalities and produced a pseudostratified epithelium on ALI but gave only 100 sparse ciliogenesis. This limited differentiation capacity may be explained by reports 101 that *hTERT*, following long-term growth in culture, up-regulates expression of the 102 potent mitogen c-Myc, so promoting entry into the cell cycle (21) thereby impeding 103 ciliogenesis.

104 We hypothesised that BMI-1 transduction alone may overcome these issues

105 observed with *Bmi-1+hTERT*, to produce basal cells with the potential for extended

106 proliferation that retain their differentiation capacity on ALI. In this study, BMI-1

107 transduced primary basal epithelial cells from CF and healthy donors were

108 investigated for their morphology, growth characteristics and karyotype. We also

109 assessed the cells mucociliary differentiation potential at ALI along with their Na⁺ and

110 Cl⁻ transport properties in Ussing chamber studies. We then demonstrate their use

111 for the production of novel engineered disease models by shRNA knockdown of

112 DNAH5, a gene associated with PCD, a ciliopathy with significant lung pathology

113 resulting from abnormal mucociliary clearance. BMI-1 transduction offers a facile

114 method to greatly extend the utility of basal epithelial cells for translational and basic

115 research.

116

117 MATERIALS & METHODS

118 Materials

- 119 Primary antibodies used in this study can be found in Table 1. Secondary antibodies
- 120 for immunofluorescence were anti-IgG antibodies conjugated with AlexaFluor dyes
- 121 (Invitrogen, Life Technologies). Secondary antibodies for Western blots were
- 122 horseradish peroxidase-conjugated (HRP-conjugated) anti-IgG antibodies (Dako,
- 123 Agilent Technologies).

124 Collagen Coating

- 125 Tissue culture flasks and transwells were coated for 1 hour at room temperature with
- 126 1% (v/v) solution of a 3mg/mL bovine collagen solution (PureCol; Advanced
- Biomatrix) in phosphate buffered saline (PBS), then washed with distilled water andair-dried.

129 Cell Culture

- 130 HEK293T cells were cultured in Dulbecco's Modified Eagle Medium (DMEM)
- 131 supplemented with 10% (v/v) foetal bovine serum. Normal human bronchial epithelial
- 132 (NHBE) cells, cystic fibrosis human bronchial epithelial cells (CFBE) cells were
- 133 grown on collagen-coated plastic in bronchial epithelial growth media (BEGM;
- 134 Lonza). All cells were grown at 37°C and 5% CO₂. NHBE and CFBE cells were
- 135 purchased from Lonza and Epithelix SàRL.

136 Lentivirus Production and Transduction

- 137 Full-length human BMI-1 cDNA was PCR cloned from pHR-EF1α-BMI1-IRES-GFP
- 138 plasmid(20) with Xhol and BamHl sites added and TOPO cloned into pCR4 TOPO
- 139 vector before being subcloned into pLVX-Puro vector digested with *Xhol* and *BamHI*.
- 140 Lentivirus was produced as previously described(20), concentrated by centrifugation

- 141 at 4,500 x g for 18 hours at 4°C, re-suspended in OptiMem and added to cell media
- 142 to transduce NHBE and CFBE cells (Lonza) at passage 2.

143 **Doubling Time Analysis**

- 144 NHBE and NHBE BMI-1 cells at varying passage numbers were seeded at densities
- 145 of 30,000 cells per well onto collagen-coated 12-well plates. Cells were detached
- using trypsin-EDTA following 1-4 days in culture and total cell numbers per well were
- 147 counted using a haemocytometer. An online calculator was used to calculate the
- 148 doubling time (Roth V. 2006 Doubling Time Computing, Available from:
- 149 <u>http://www.doubling-time.com/compute.php</u>). Doubling times were calculated using
- 150 the formula;

$$doubling \ time = \frac{duration \ \times \ \log(2)}{\log(final \ cell \ count) - \log(initial \ cell \ count)}$$

151 Where cell count values were mean cell count of 3 independent wells.

152 Western Blotting

- 153 Cells were lysed with Cell Extraction Buffer (Life Technologies), boiled in the
- 154 presence of NuPage LDS Sample Buffer (Life Technologies) and loaded onto
- 155 NuPage Novex 4-12% Bis-Tris gels (Life Technologies). Electrophoresis and protein
- 156 transfer onto Immobilon-P polyvinylidene fluoride membranes were performed using
- 157 standard protocols. Antibodies against BMI-1, p16Ink4a and GAPDH and
- 158 appropriate HRP-conjugated secondary antibodies were used for probing with bands
- 159 visualised using Pierce ECL Western Blotting Substrate (Life Technologies, Paisley,
- 160 UK) and a UVIchemi chemiluminescence imaging system (UVItec).

161 Air-liquid Interface (ALI) Culture

162 Cells grown to ~80% confluence in T75 flasks were trypsinised, seeded at a density

163 of 900,000 cells/cm² on Transwell inserts (Corning) and grown at an ALI as

164 previously described(8). Cell were maintained at an ALI for 4 weeks before analyses

165 were performed.

166 **Quantitative Reverse Transcription PCR (qRT-PCR)**

167 Unless indicated, all reagents for qRT-PCR were obtained from ThermoFisher. Total

168 RNA was harvested from cells using RNeasy Mini Kit (Qiagen) and potential DNA

169 impurities digested using DNase I enzyme (TURBO DNA-free kit). Purified RNA was

170 reverse transcribed with 2.5U/µL murine leukaemia virus (MuLV) reverse

171 transcriptase at 42°C for 1 hour in a reaction containing 1x GeneAmp PCR Gold

172 Buffer, 1mM each dNTP, 5 μ M random hexamers, 5mM MgCl₂ and 1U/ μ L RNase

173 inhibitor. The resulting cDNA was used in a qPCR reaction containing 1x Platinum

174 Quantitative PCR SuperMix-UDG w/ROX and 1x TaqMan Gene Expression Assay

primer/probe set (GAPDH primer/probe set Hs99999905_m1; DNAH5 primer/probe

176 set Hs00292485_m1). The PCR reaction cycles used were 50°C for 2 minutes, 95°C

177 for 10 minutes, 40 cycles of 95°C for 15 seconds and 60°C for 1 minute on an ABI

178 PRISM 7000 Sequence Detection System (Applied Biosystems). Fluorescence data

179 was collected at the end of each 60°C reaction and relative expression levels

180 calculated using the delta-delta Ct (2- $\Delta\Delta$ Ct) method(19).

181 Immunofluorescence Staining and Confocal Microscopy

182 Cells were fixed with 4% PFA for 10 minutes at room temperature, washed with PBS

and permeabilised with PBS-Triton (PBS 0.1% (v/v) Triton-X100) for 10 minutes at

184 room temperature before blocking, immunostaining and mounting on microscope

185 slides as previously described(26). Images were obtained using an Inverted Zeiss

LSM 710 Confocal microscope with the appropriate excitation lasers selected for thedyes used.

188 Fluorescence Microscopy

- 189 Bright-field and fluorescence images were captured with a Nikon Digital Sight DS-
- 190 QiMC video camera attached to a Nikon Eclipse Ti-U inverted microscope. Videos
- and images were processed using NIS Elements AR software (Nikon, v4.00.12).

TEM for Cilia Ultrastructure

- 193 Ciliated cells cultured at an ALI were scraped and cells washed off with 200µL
- 194 warmed BEBM. Cells were fixed by addition of 2mL of 2.5% glutaraldehyde and
- 195 stored at 4°C for at least 24 hours prior to further processing as previously
- 196 described(24). Assessment of cilia ultrastructure was undertaken blinded by Dr
- 197 Amelia Shoemark, a member of the PCD diagnostic service team at the Royal
- 198 Brompton & Harefield NHS Foundation Trust, UK.

199 High-Speed Video Microscopy

- 200 High-speed video was recorded using a MotionPro X4 high-speed motion camera
- attached to a Nikon Eclipse Ti-U inverted microscope built with an environmental
- 202 chamber. Videos were recorded at a frame rate of 500fps using Motion Studio
- software (IDT Vision, v2.11) with cells maintained at 37°C.
- 204 For cilia beat frequency (CBF) assessment, ALI cultures were washed twice with
- 205 PBS to remove mucus that may have affected CBF. After washing, the cells were
- allowed to equilibrate at 37°C and 5% CO₂ for 20 minutes before video recording. At
- 207 least four independent cultures per donor line were videoed with five areas recorded
- 208 per culture, i.e., at least 20 videos were captured per donor line. To minimise bias

209 videos were recorded from the top, bottom, left, right and centre region of each

210 culture and cilia beat-frequency assessed using CiliaFA software(25).

211 Electrophysiology Studies

212 Cells were grown at ALI for 4 weeks on Snapwell membranes (Corning) to enable

213 mucociliary differentiation. Snapwells were then mounted on Ussing chambers and

short circuit current (lsc) was measured as previously described (32). Briefly,

215 monolayers were mounted in Ussing chambers in physiological salt solution

consisting of 117mM NaCl, 25mM NaHCO3, 4.7mM KCl, 1.2mM MgSO4, 1.2mM

217 KH2PO4, 2.5mM CaCl2 and 11mM d-glucose. The solution was continuously

circulated throughout the course of the experiment and maintained at 37°C whilst

bubbled with 21% O_2 + 5% CO_2 premixed gas. Monolayers were first maintained

220 under open-circuit conditions until transepithelial potential difference (Vt) and

221 resistance stabilised. The cells were then short-circuited by clamping V_t at 0 mV

using a DVC-4000 voltage/current clamp, and lsc was measured and recorded using

a PowerLab computer interface. Every 30 seconds the preparations were returned to

224 open-circuit conditions for 3 seconds so that the spontaneous V_t could be measured

and trans-epithelial electrical resistance (TEER) calculated. Drugs were circulated in

226 physiological salt solution and added in the order of amiloride (10 μM, apical),

forskolin (25 μ M, apical and basolateral) and GlyH-101 (10 μ M, apical).

228 **RESULTS**

229 Characterisation of BMI-1 transduced cells in submerged culture

230 Primary NHBE cells maintained in submerged cultures displayed a 231 characteristic cobblestone appearance (Figure 1a) but by passage 3 cells became 232 elongated in appearance (white arrow; Figure 1b) and squamous differentiation was 233 evident (black arrow; Figure1b). In contrast, BMI-1 transduced NHBE cells (NHBE-234 BMI-1) maintained their cobblestone appearance following extensive passaging, for 235 example at passage 11 (Figure 1c) and passage 17 (Figure1d). However, squamous 236 cells became evident following 25 passages (Figure 1e) after which the cells 237 senesced, with no observable cell division for ten days. The cells maintained a 238 normal diploid karyotype even at passage 23 (Figure 2). 239 BMI-1 down-regulates expression of the pro-senescent protein p16lnk4A. NHBE 240 cells transduced with BMI-1 had low levels of p16Ink4A protein and high levels of 241 BMI-1 (Figure 3a). Levels of BMI-1 in untransduced NHBE cells declined with an 242 increase in passaging whilst levels of p16Ink4A increased and were higher in 243 senesced, untransduced NHBE cells at passage 6 while BMI-1 expression was not 244 evident by Western blot (Figure 3a).

SV40 large T-antigen or ROCK inhibition extends the replication potential of basal cells but alters the proliferation rate of the cells(4, 7, 12) therefore we assessed the doubling times of BMI-1 transduced cells at different passages (Figure 3b). We determined that untransduced cells at passage 2 had a doubling time of 1.18 days similar to BMI-1 transduced cells at passages 12 and 15 (doubling times of 1.25 and 1.21 days respectively) although by passage 23 the doubling time had increased to 1.49 days, consistent with observations of senescence at passage 25.

252 **Differentiation of NHBE-BMI-1 Cells**

253 NHBE-BMI-1 basal cells were subsequently analysed for their differentiation 254 potential when cultured at ALI. After 2 -3 weeks culture, both primary NHBE and 255 NHBE-BMI-1 cells produced motile cilia (Video 1a and b respectively). NHBE-BMI-1 256 cells maintained the ability to differentiate and produce cilia even at passage 15.

To quantify cilia function, we assessed cilia beat frequency of both primary and BMI-1 transduced NHBE and CFBE cells. Beating cilia from CFBE cells could not be detected, most likely due to the build-up of viscous mucus hindering cilia beating, until cultures were washed. As such, CFBE and NHBE cultures were washed twice prior to video recording and CBF analysis as detailed in the methods section.

CBF analysis of both primary and BMI-1 transduced NHBE and CFBE cells showed mean values within the normal range for respiratory cilia of 9-17Hz(25) (Figure 4a and b). Primary NHBE and NHBE-BMI-1 cells had a CBF of 16.7±0.2Hz and 15.3±0.2Hz respectively (Figure 4a) and primary CFBE and CFBE-BMI-1 cells exhibited CBF values of 12.9±0.3Hz and 14.3±0.3Hz respectively.

267 Further evidence of differentiation was demonstrated by immuno-detection, in 268 NHBE-BMI-1 cells, of the tight junction protein occludin (Figure3c) and the mucins 269 MUC5AC and MUC5B (Figure 4d, e). In addition, basal cells were present and 270 indicated by p63 staining (Figure 4f) and BMI-1 protein was present in all nuclei 271 (Figure 4g). The ciliary protein acetylated α -tubulin was also detected by 272 immunostaining and highlighted abundant ciliation (Figure 4h). Further analysis of 273 the cilia in differentiated NHBE-BMI-1 cells by TEM showed that they had a normal 274 9+2 ultrastructure with both inner and outer dynein arms present (Figure 4i, Table 2 275 and Table 3).

276 *Electrophysiology studies*

277 Primary HBE cells grown on ALI develop a trans-epithelial electrical 278 resistance (TEER) with ion transport properties that can be measured by mounting of 279 cultured epithelia on Ussing chambers and addition of drugs that can activate or 280 inhibit specific cell surface ion channels. Cultures of primary NHBE cells from two different donors showed baseline TEER values of $331.1\pm105.5\Omega$.cm² and 281 $621.0\pm33.2\Omega$.cm² (Table 4) and primary CFBE cells developed TEER of 282 283 1307.9±36.6Ω.cm². Similarly, *BMI-1* transduced NHBE and CFBE cells developed high TEER when grown at an ALI (1268.4 \pm 78.4 Ω .cm² and 917.6 \pm 165.3 Ω .cm² 284 285 respectively; Table 4) demonstrating the cells retained their ability to form an 286 electrically resistive epithelium.

287 Short circuit current (Isc) analysis in Ussing chambers of NHBE and CFBE cells 288 revealed that both primary NHBE cells and passage 13 NHBE-BM-1 cells cultured at 289 ALI also had similar electrophysiology. Amiloride (10µM), an inhibitor of the epithelial 290 Na^{+} channel ENaC reduced I_{sc} in all cultures, although the amiloride-sensitive I_{sc} was 291 variable. Subsequent elevation of cellular cAMP with forskolin (25µM) increased Isc 292 and this elevation was inhibited by the CFTR inhibitor Gly-H101 (10 μ M) (Figure 5 a, 293 b). Thus, ENaC and CFTR-mediated ion transport was retained in NHBE-BMI-1 294 cells. Primary CFBE cells and passage 17 CFBE BMI-1 cells cultured at ALI also 295 exhibited amiloride-inhibitable I_{sc} but no response to either forskolin or GlyH-101 was 296 observed, as expected due to the lack of CFTR in these cells (Figure 5 c, d). Thus, 297 CFBE-BMI-1 cells, like NHBE-BMI-1, also maintain the Na+ and CI- ion transport 298 characteristics of non-transduced primary CF cells.

299 Use of BMI-1 transduced cells to generate PCD cell models

We next explored the potential use of the BMI-1 transduced NHBE cells to generate an in vitro model of PCD. The outer dynein arm protein *DNAH5* is the most commonly mutated gene but even so this is a rare disease and cells are often not readily available. Cells with *DNAH5* mutations lack the DNAH5 protein in the ciliary axoneme and have missing outer dynein arms (ODAs) (13). NHBE cells transduced with BMI-1 were additionally transduced with a DNAH5 shRNA lentiviral construct that also expresses green fluorescent protein (GFP).

307 *DNAH5* expression in shRNA-transduced cells was silenced by approximately 75%
 308 relative to untransduced cells (Figure 6a) while scrambled shRNA had no effect on
 309 *DNAH5* expression indicating silencing specificity.

310 NHBE-BMI-1 cells transduced with the two shRNAs were subsequently cultured at

311 ALI to promote differentiation and ciliation. Following mucociliary differentiation,

312 NHBE-BMI-1 GFP-positive cells, transduced with scrambled shRNA had motile cilia,

313 (Video 2a) whereas GFP-positive DNAH5 shRNA silenced cells had immotile cilia

314 (Video 2b). However, in GFP negative cells (and by extension also DNAH5 shRNA

315 negative) motile cilia were still observed (Video 2c).

316 In untransduced NHBE BMI-1 cells and those GFP-positive cells transduced with the

317 scrambled shRNA, DNAH5 was localised to the ciliary axoneme in all ciliated cells

318 assessed as shown by co-localisation with acetylated α-tubulin expression. In

319 contrast, in DNAH5 shRNA transduced GFP-positive cells, only 2.9% (5/173) of

320 ciliated cells had DNAH5 in the ciliary axoneme (Figure 6b and Table 5).

321

322

323 **DISCUSSION**

324 Airway diseases are a significant cause of morbidity and mortality. Mucociliary 325 differentiation of primary airway epithelial cells using ALI culture methods provides 326 an *in vitro* model that faithfully recapitulates the *in vivo* airway epithelium for the 327 study of disease pathology and therapies. However, these cells can only be cultured 328 for 2-3 passages before they lose their ability to differentiate(5). This has important 329 practical, ethical and cost implications for research in the field. Traditional cell 330 transformation methods, using viral oncogenes that promote entry into the cell cycle, 331 produce immortal cell lines incapable of mucociliary differentiation most likely due to 332 their inability to suspend cell division and allow cilia production and differentiation.

We have shown that prevention of cellular senescence by expression of *BMI-1* allows extended passaging of HBE cells from CF and non-CF donors. Western blot analysis highlighted that senescent primary NHBE cells had accumulated high levels of the pro-senescent protein p16^{lnk4a} in agreement with other studies (1, 6, 20). *BMI-1* transduced cells, however, showed low levels of p16^{lnk4a} thereby delaying cell senescence as reported previously(15).

339 In addition to exhibiting delayed senescence, BMI-1 transduced cells retained their 340 phenotype, karyotype, ion transport characteristics cell and mucociliary 341 differentiation potential with abundant ciliation observed when cultured at ALI. Ussing 342 chamber studies revealed that, like primary HBE cells, *BMI-1* transduced NHBE and 343 CFBE cells formed electrically resistive cultures and the direction of change in Isc 344 was as expected upon addition of amiloride, forskolin and the CFTR inhibitor Gly-345 H101. We note that baseline TEER values varied between HBE donors as did the 346 magnitude of change in Isc upon addition of amiloride, forskolin and the CFTR

inhibitor Gly-H101. Such variation has also been observed by Tosoni et al. (29) who recently demonstrated baseline TEER values ranged from 309 to 2963 Ω .cm² in ALI cultures generated from the cells of 18 healthy donors.

350 In agreement with our findings, Torr et al(28) recently demonstrated that 351 transduction of basal cells, from different two donors, with human BMI-1 alone 352 extends the proliferative potential of NHBE cells whilst retaining their differentiation 353 potential as demonstrated by immunostaining and scanning electron microscopy. 354 Our study extends on these findings demonstrating that passaging capacity of 355 diseased cells (CFBE) can also be extended using this method. Taken together this 356 would suggest BMI-1 transduction of bronchial epithelial cells permits extended 357 passaging and mucociliary differentiation independent of donor and/or disease status 358 although further studies are needed to confirm this.

359 BMI-1 transduction did not immortalise the HBE cells in contrast to viral antigens 360 such as the SV40 large T-antigen used to produce the 16HBE14o- cell line(5). 361 However, BMI transduced cells could still be differentiated at 20-25 passages 362 representing a significant advantage of this method over use of viral antigens. Using 363 the ALI culture protocol outlined in the current study one can routinely obtain from 6-364 8 functional epithelial transwells in a 24-well ALI culture format per passage enabling 365 the generation of a minimum of ~90-100 transwells from a single donor. This is 366 significantly higher than the 10-15 epithelial transwells that can be generated with ~1x10⁶ primary bronchial epithelial cells (typical quantity obtained from commercial 367 368 providers) or brushing of the nasal turbinate of a single donor(29). Furthermore, sub-369 culturing of BMI-1 transformed cells, as opposed to seeding ALI cultures, would 370 enable banking of early passage cells and the potential to generate exponentially 371 more functional epithelia at each passage.

372 Tosoni et al. (29) recently demonstrated that ALI cultures generated from different 373 healthy donors can yield epithelia with vastly different physiological properties and 374 drug responses. The BMI-1 transduction protocol enables the generation of a large 375 number of epithelia generated from donors with similar genetic backgrounds, or 376 indeed from a single donor, allowing the study of disease pathophysiology in a 377 manner that avoids the influence of genetic variability in cells from different donors. 378 This highlights the potential for the development of personalised treatments using 379 BMI-1 transduced cells.

380 In addition, an extended passaging capacity affords the opportunity for modification 381 of HBE cells to create new models, to better understand disease and find novel 382 treatments. As a proof of concept, we transduced NHBE BMI-1 cells with shRNA 383 targeted against DNAH5 in an attempt to create a model of PCD. The shRNA 384 construct contained a GFP reporter to allow for selection of cells in which the DNAH5 385 shRNA was expressed. Focussing on cells expressing GFP, we demonstrated loss 386 of ciliary motility and absence of DNAH5 in the ciliary axoneme of cells transduced 387 with the DNAH5 targeted shRNA so mimicking the phenotype seen in patient 388 cells(13). shRNA-mediated knockdown has been previously used to model PCD in 389 otherwise healthy primary HBE cells (10, 11, 17) but these cells were not long lived 390 so could not be used for further study to assess, for example, protein interactions or 391 novel treatments. Gene addition, shRNA knockdown, or genome editing of BMI-1 392 transduced HBE cells could therefore provide a more useful tool for the study of a 393 number of airway diseases.

Recently the use of pharmacological Rho-kinase inhibition along with co-culture of HBE cells with irradiated feeder-layer fibroblasts has been described to allow indefinite passage of HBE cells whilst retaining the cells differentiation capacity when

397 placed at ALI (18, 27). However, studies where the mucociliary differentiation 398 potential of CRCs have been assessed have not reported successful mucociliary 399 differentiation beyond passage 11(2, 22, 27). Furthermore, CRC morphology and 400 doubling times differ significantly to their parent cells with CRC cells being smaller 401 and growing in colonies as well as showing faster proliferation rates(18, 27). 402 Following viral transduction, BMI-1 expressing NHBE and CFBE cells are cultured 403 exactly as non-transformed primary cells, without the need for a feeder layer, a factor 404 that is likely to aid in the rapid uptake of this method of transformation and 405 dissemination of the resulting cell models between laboratories and in the 406 maintenance of cells in biobanks.

407 In summary, here we have shown that *BMI-1* transduction delays senescence in 408 HBE cells from healthy and CF donors whilst maintaining the cells mucociliary 409 differentiation potential. We have undertaken extensive characterisation of the 410 differentiated cells showing normal ciliary beat frequency and ciliary ultrastructure. 411 Ussing chamber studies with BMI-1 transformed NHBE and CFBE cells showed that 412 these cells exhibit similar Na+ and CI- ion transport characteristics to their respective 413 primary cells, validating their use as models of CF. Furthermore, we have 414 demonstrated how BMI-1- transduced cells can be engineered by further 415 transduction with DNAH5 shRNA to recapitulate an in vitro disease model of primary 416 ciliary dyskinesia, a valuable feature when studying rare diseases such as PCD 417 where patient samples are difficult to obtain.

418

419

Brookes S, Rowe J, Gutierrez Del Arroyo A, Bond J, and Peters G. Contribution
of p16(INK4a) to replicative senescence of human fibroblasts. *Exp Cell Res* 298: 549-559,
2004.

Butler CR, Hynds RE, Gowers KH, Lee Ddo H, Brown JM, Crowley C, Teixeira
VH, Smith CM, Urbani L, Hamilton NJ, Thakrar RM, Booth HL, Birchall MA, De
Coppi P, Giangreco A, O'Callaghan C, and Janes SM. Rapid Expansion of Human
Epithelial Stem Cells Suitable for Airway Tissue Engineering. *Am J Respir Crit Care Med*194: 156-168, 2016.

Chu Q, Tousignant JD, Fang S, Jiang C, Chen LH, Cheng SH, Scheule RK, and
Eastman SJ. Binding and uptake of cationic lipid:pDNA complexes by polarized airway
epithelial cells. *Hum Gene Ther* 10: 25-36., 1999.

432 4. Cozens AL, Yezzi MJ, Kunzelmann K, Ohrui T, Chin L, Eng K, Finkbeiner WE,
433 Widdicombe JH, and Gruenert DC. CFTR expression and chloride secretion in polarized
434 immortal human bronchial epithelial cells. *Am J Respir Cell Mol Biol* 10: 38-47, 1994.

435 5. Cozens AL, Yezzi MJ, Kunzelmann K, Ohrui T, Chin L, Eng K, Finkbeiner WE,
436 Widdicombe JH, and Gruenert DC. CFTR Expression and Chloride Secretion in Polarized
437 Immortal Human Bronchial Epithelial Cells. *Am J Respir Cell Mol Biol* 10: 38-47, 1994.

438 6. Fulcher ML, Gabriel SE, Olsen JC, Tatreau JR, Gentzsch M, Livanos E,
439 Saavedra MT, Salmon P, and Randell SH. Novel human bronchial epithelial cell lines for
440 cystic fibrosis research. Am J Physiol Lung Cell Mol Physiol 296: 82-91, 2009.

Fulcher ML, Gabriel SE, Olsen JC, Tatreau JR, Gentzsch M, Livanos E,
Saavedra MT, Salmon P, and Randell SH. Novel human bronchial epithelial cell lines for
cystic fibrosis research. *Am J Physiol Lung Cell Mol Physiol* 296: L82-91, 2009.

444 8. Hirst RA, Rutman A, Williams G, and Callaghan CO. Ciliated Air-Liquid
445 Cultures as an Aid to Diagnostic Testing of Primary Ciliary Dyskinesia. *Chest* 138: 1441446 1447, 2010.

447 9. Hirst RA, Rutman A, Williams G, and O'Callaghan C. Ciliated air-liquid cultures
448 as an aid to diagnostic testing of primary ciliary dyskinesia. *Chest* 138: 1441-1447, 2010.

Horani A, Brody SL, Ferkol TW, Shoseyov D, Wasserman MG, Ta-shma A,
Wilson KS, Bayly PV, Amirav I, Cohen-Cymberknoh M, Dutcher SK, Elpeleg O, and
Kerem E. CCDC65 mutation causes primary ciliary dyskinesia with normal ultrastructure
and hyperkinetic cilia. *PLoS ONE* 8: e72299, 2013.

Horani A, Ferkol TW, Shoseyov D, Wasserman MG, Oren YS, Kerem B, Amirav
I, Cohen-Cymberknoh M, Dutcher SK, Brody SL, Elpeleg O, and Kerem E. LRRC6
mutation causes primary ciliary dyskinesia with dynein arm defects. *PLoS ONE* 8: e59436,
2013.

Horani A, Nath A, Wasserman MG, Huang T, and Brody SL. Rho-Associated
Protein Kinase Inhibition Enhances Airway Epithelial Basal-Cell Proliferation and Lentivirus
Transduction. *Am J Respir Cell Mol Biol* 49: 341-347, 2013.

460 13. Hornef N, Olbrich H, Horvath J, Zariwala MA, Fliegauf M, Loges NT,
461 Wildhaber J, Noone PG, Kennedy M, Antonarakis SE, Blouin JL, Bartoloni L, Nusslein
462 T, Ahrens P, Griese M, Kuhl H, Sudbrak R, Knowles MR, Reinhardt R, and Omran H.

- 463 DNAH5 Mutations Are a Common Cause of Primary Ciliary Dyskinesia With Outer Dynein 464 Arm Defects. *Am J Respir Crit Care Med* 174: 120-126, 2006.
- 465 14. Hussain S, Ji Z, Taylor AJ, DeGraff LM, George M, Tucker CJ, Chang CH, Li
 466 R, Bonner JC, and Garantziotis S. Multiwalled Carbon Nanotube Functionalization with

467 High Molecular Weight Hyaluronan Significantly Reduces Pulmonary Injury. ACS Nano 10:
468 7675-7688, 2016.

469 15. Jacobs JJ, Kieboom K, Marino S, DePinho RA, and van Lohuizen M. The
470 oncogene and Polycomb-group gene bmi-1 regulates cell proliferation and senescence
471 through the ink4a locus. *Nature* 397: 164-168, 1999.

Kesimer M, Kirkham S, Pickles RJ, Henderson AG, Alexis NE, Demaria G,
Knight D, Thornton DJ, and Sheehan JK. Tracheobronchial air-liquid interface cell
culture: a model for innate mucosal defense of the upper airways? *Am J Physiol Lung Cell Mol Physiol* 296: L92-L100, 2009.

- Li Y, Yagi H, Onuoha EO, Damerla RR, Francis R, Furutani Y, Tariq M, King
 SM, Hendricks G, Cui C, Saydmohammed M, Lee DM, Zahid M, Sami I, Leatherbury
 L, Pazour GJ, Ware SM, Nakanishi T, Goldmuntz E, Tsang M, and Lo CW. DNAH6
- and Its Interactions with PCD Genes in Heterotaxy and Primary Ciliary Dyskinesia. *PLoS Genet* 12: e1005821, 2016.
- Liu X, Ory V, Chapman S, Yuan H, Albanese C, Kallakury B, Timofeeva OA,
 Nealon C, Dakic A, Simic V, Haddad BR, Rhim JS, Dritschilo A, Riegel A, McBride A,
 and Schlegel R. ROCK inhibitor and feeder cells induce the conditional reprogramming of
 epithelial cells. *Am J Pathol* 180: 599-607, 2012.
- 485 19. Livak KJ, and Schmittgen TD. Analysis of relative gene expression data using real486 time quantitative PCR and the 2(-Delta Delta C(T)) Method. *Methods* 25: 402-408, 2001.
- 487 20. McKay TR, Camarasa MV, Iskender B, Ye JP, Bates N, Miller D, Fitzsimmons
 488 JC, Foxler D, Mee M, Sharp TV, Aplin J, Brison DR, and Kimber SJ. Human feeder cell
 489 line for derivation and culture of hESc/hiPSc. *Stem Cell Res* 7: 154-162, 2011.
- 490 21. Milyavsky M, Shats I, Erez N, Tang X, Senderovich S, Meerson A, Tabach Y,
 491 Goldfinger N, Ginsberg D, Harris CC, and Rotter V. Prolonged culture of telomerase492 immortalized human fibroblasts leads to a premalignant phenotype. *Cancer Res* 63: 7147493 7157, 2003.
- 494 22. Reynolds SD, Rios C, Wesolowska-Andersen A, Zhuang Y, Pinter M, Happoldt
 495 C, Hill CL, Lallier SW, Cosgrove GP, Solomon GM, Nichols DP, and Seibold MA.
 496 Airway Progenitor Clone Formation is Enhanced by Y-27632-dependent Changes in the
 497 Transcriptome. Am J Respir Cell Mol Biol 2016.
- 498 23. Rousseau K, Wickstrom C, Whitehouse DB, Carlstedt I, and Swallow DM. New
 499 monoclonal antibodies to non-glycosylated domains of the secreted mucins MUC5B and
 500 MUC7. *Hybridoma and Hybridomics* 22: 293-299, 2003.
- 501 24. Shoemark A, Dixon M, Beales PL, and Hogg CL. Bardet Biedl Syndrome Motile
 502 Ciliary Phenotype. *Chest* 147: 764-770, 2015.
- 503 25. Smith CM, Djakow J, Free RC, Djakow P, Lonnen R, Williams G, Pohunek P,
- Hirst RA, Easton AJ, Andrew PW, and O'Callaghan C. ciliaFA: a research tool for
 automated, high-throughput measurement of ciliary beat frequency using freely available
 software. *Cilia* 1: 14, 2012.
- Smith CM, Kulkarni H, Radhakrishnan P, Rutman A, Bankart MJ, Williams G,
 Hirst RA, Easton AJ, Andrew PW, and O'Callaghan C. Ciliary dyskinesia is an early
 feature of respiratory syncytial virus infection. *Eur Respir J* 43: 485-496, 2014.
- 510 27. Suprynowicz FA, Upadhyay G, Krawczyk E, Kramer SC, Hebert JD, Liu X, 511 Yuan H, Cheluvaraju C, Clapp PW, Boucher RC, Jr., Kamonjoh CM, Randell SH, and 512 Schlegel R. Conditionally reprogrammed cells represent a stem-like state of adult epithelial 513 cells. *Proc Natl Acad Sci U S A* 109: 20035-20040, 2012.
- 514 28. Torr E, Heath M, Mee M, Shaw D, Sharp TV, and Sayers I. Expression of
 515 polycomb protein BMI-1 maintains the plasticity of basal bronchial epithelial cells.
- 516 Physiological Reports 4: e12847, 2016.

- 517 29. **Tosoni K, Cassidy D, Kerr B, Land SC, and Mehta A**. Using Drugs to Probe the 518 Variability of Trans-Epithelial Airway Resistance. *PLoS ONE* 11: e0149550, 2016.
- 519 30. Wong AP, Bear CE, Chin S, Pasceri P, Thompson TO, Huan LJ, Ratjen F, Ellis 520 J, and Rossant J. Directed differentiation of human pluripotent stem cells into mature
- 521 airway epithelia expressing functional CFTR protein. *Nat Biotechnol* 30: 876-882, 2012.
- 31. Wong AP, and Rossant J. Generation of Lung Epithelium from Pluripotent Stem
 Cells. *Curr Pathobiol Rep* 1: 137-145, 2013.
- 524 32. Woollhead AM, Sivagnanasundaram J, Kalsi KK, Pucovsky V, Pellatt LJ, Scott
- 525 JW, Mustard KJ, Hardie DG, and Baines DL. Pharmacological activators of AMP-
- activated protein kinase have different effects on Na+ transport processes across human lung
- 527 epithelial cells. *Br J Pharmacol* 151: 1204-1215, 2007.
- 528

530 AUTHOR CONTRIBUTIONS

531 M.M.M., A.S., R.A.H., J.M.D. and D.L.B. contributed to data collection. All authors 532 contributed to study design, data analysis, interpretation of the data and critical 533 revision of the final manuscript. All authors approved the final version of the 534 manuscript.

535 **GRANTS**

- 536 This study was funded by the Great Ormond Street Hospital Children's Charity
- 537 (GOSHCC), the Child Health Research Appeal Trust (CHRAT) and supported by the
- 538 National Institute for Health Research Biomedical Research Centre at Great Ormond
- 539 Street Hospital for Children NHS Foundation Trust and University College London.

540 **DISCLOSURES**

- 541 The authors declare no competing financial interests.
- 542

544 ADDITIONAL INFORMATION

545 Supplementary videos available.

546 **FIGURE LEGENDS**

547 Figure 1. BMI-1 maintains healthy cell morphology in 2D culture.

548 The morphology of (a) NHBE cells at passage 1 and (b) passage 3 was observed

- 549 under light microscopy and compared to NHBE BMI-1 cells after passages (c) 11, (d)
- 550 17 and (e) 25. White arrows highlight elongated cells and black arrows highlight
- 551 squamous cells. Scale bars are 100µm.

552 Figure 2. Karyotype analysis of NHBE-BMI-1 cells.

553 Karyotype of passage 23 NHBE-BMI-1 cells was undertaken by The Doctors 554 Laboratory, London.

555 Figure 3. Elevated p16^{lnk4a} precedes senescence and BMI-1 functions by 556 inhibiting p16^{lnk4a} and retains a normal cell doubling time.

- 557 (a) Western blot was used to assess levels of BMI-1 and p16^{lnk4A} in serially
- 558 passaged NHBE cells and BMI-1 transduced cells and (b) cell counting was used to
- 559 determine the replication kinetics of NHBE and NHBE BMI-1 cells at varying
- 560 passages. Growth curves are presented as percent of mean of day 1 cell count. Data
- are mean \pm S.E.M. For each data point n=3 biological replicates.

562 Figure 4. BMI-1 cells retain their mucociliary differentiation capacity.

- 563 Extensively passaged BMI-1 transduced cells (passage 15) were differentiated on
- 564 ALI and cilia beat frequency of (a) NHBE and (b) CFBE cells was determined using
- 565 ciliaFA plugin(25) for ImageJ. Data are mean ± S.E.M; n= 4 independent ALI
- 566 cultures, 5 fields videoed per culture. Immunostaining of NHBE-BMI-1 cells was used
- 567 to show tight junction formation (occludin; c), mucin production (MUC5AC and
- 568 MUC5B; d and e respectively), the presence of basal cells (p63+; f), widespread
- 569 BMI-1 expression (BMI-1; g), and extensive ciliation (acetylated α -tubulin; h). TEM
- 570 was used to determine cilia ultrastructure (i). Images are representative of 4
- 571 independent ALI cultures per marker. Scale bars for c-h are 50µm and 100nm for i.

572 Figure 5. BMI-1 cells form ALI cultures suitable for Ussing chamber studies.

- 573 Representative Ussing chamber traces and changes in short-circuit current (I_{sc}) in
- 574 response to administration of amiloride (apical), forskolin (apical and basolateral) and
- 575 GlyH-101 (apical) in primary and BMI-1 transduced (a and b) NHBE and (c and d)
- 576 CFBE cells are shown. Data are mean ± S.E.M; n= at least 3 independent ALI
- 577 cultures (see Table 4 for exact values).

578 Figure 6. DNAH5 knockdown recapitulates PCD phenotype.

- 579 (a) qRT-PCR was used to assess DNAH5 mRNA expression in NHBE-BMI-1 cells
- 580 and NHBE BMI-1-transduced with lentivirus expressing either a scrambled or

- 581 *DNAH5*-targetting shRNA and grown in submerged 2D culture. **P<0.01; one-way
- 582 ANOVA with Bonferroni's post-test used to assess significance. Data are mean ±
- 583 S.E.M. (b) Immunostaining for DNAH5 and acetylated α -tubulin was used to assess
- 584 the presence or absence of DNAH5 in the ciliary axoneme of shRNA transduced and
- 585 untransduced NHBE BMI-1 cells differentiated at ALI. Presence of GFP fluorescence
- 586 denotes cells transduced with the GFP-shRNA construct and so expressing the
- 587 shRNA. Scale bars are 20µm. Images are representative of 4 independent ALI
- 588 cultures per condition.

TABLES

Table 1. Primary antibodies used in this study.

Name	Supplier	Dilution WB/IF		
Anit-MUC5AC	Life Technologies	NA/1:100		
Anti-Acetylated α- tubulin	Sigma-Aldrich	NA/1:500		
Anti-BMI-1	Life Technologies	1:200/1:100		
Anti-GAPDH	Life Technologies	1:1000/1:500		
Anti-MUC5B	Kind gift from Professor Dallas Swallow(23)	NA/neat		
Anti-Occludin	Invitrogen, Life Technologies	NA/1:100		
Anti-p16 ^{INK4}	Pharmingen, BD Biosciences	1:200/NA		
Anti-p63	Invitrogen, Life Technologies	NA/1:100		

Table 2. Microtubule organisation of motile cilia.

Microtubule Organisation	Frequency (%)
Normal 9+2	92.05
Central Pair Defect	0.66
Disarranged	3.31
Other Defect	3.97

Table 3. Dynein arm presence in motile cilia.

Dynein Arms	Frequency (%)		
ODA and IDA Present	100.00		
ODA Only	0.00		
IDA Only	0.00		
ODA and IDA Absent	0.00		

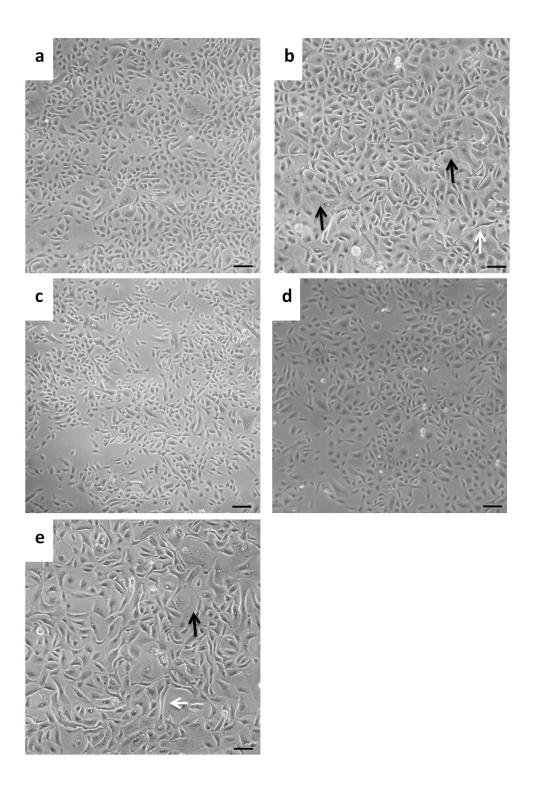
 Table 4. Trans-epithelial electrical resistance (TEER) measurements.

Name	Passage	TEER (Ω.cm ² ±S.E.M)	n
NHBE (AB053901)	P1	621.0 ± 33.2	5
NHBE (AB037501)	P1	331.1 ± 105.5	3
NHBE BMI-1	P13	1268.4 ± 78.4	4
CFBE	P2	1307.9 ± 36.6	5
CFBE BMI-1	P17	917.6 ± 165.3	6

602

Table 5. DNAH5 localisation.

	Is DNAH5 located in ciliary axoneme?		
shRNA Target	Yes	No	
Untransduced	157	0	
Scrambled	147	0	
DNAH5	5	173	



	820	- HORES	×		Barren de
STREET, ST	X	Sector Sector		A second	and a second
-diame	1000	44800 15	IL WELL	900 juli	1000
88	840 2 20	ñ,á	5.8	×	ŧ

